# Wash–Dry Cycle Induced Changes in Low-Ordered Parts of Regenerated Cellulosic Fibers

**Barbora Široká,[1] Avinash P. Manian,[1] Michael F. Noisternig,[2] Ute Henniges,[3] Mirjana Kostic,[3] Antje Potthast,[3] Ulrich J. Griesser,[2] Thomas Bechtold[1]**

[1]*Christian Doppler Laboratory for Textile and Fibre Chemistry in Cellulosics, Research Institute of Textile Chemistry and Textile Physics, Leopold-Franzens University of Innsbruck, A-6850 Dornbirn, Austria*
[2]*Department of Pharmaceutical Technology, Institute of Pharmacy, Leopold-Franzens University of Innsbruck, A-6020 Innsbruck, Austria*
[3]*Christian-Doppler-Laboratory, "Advance Cellulose Chemistry and Analytics," Department of Chemistry, Biopolymer Analytics, University of Agricultural Sciences Vienna, A-1190 Vienna, Austria*

Received 5 February 2011; accepted 26 January 2012
DOI 10.1002/app.36894
Published online in Wiley Online Library (wileyonlinelibrary.com).

**ABSTRACT:** Three regenerated cellulosic fiber types: lyocell, viscose, and modal were subjected to repetitive wet–dry treatments. Simulated treatments showed reorganization of the internal fiber structure which could be determined by accessibility studies. The reduction in liquid water retention capacity was found to be greater for lyocell than that for modal and viscose, sorption of iodine, and water vapor reduced for all studied fibers. The wet–dry treatment did not have influence on chemical reactivity of cellulosic fibers characterized by complexation of iron under highly alkaline conditions. The effect of wet–dry treatment on the tenacity, elongation at break, abrasion resistance, and molecular weight distribution of fibers was also explored in this study. The reduced strength in treated specimens was not accompanied by changes in molecular weight distributions. Based on these results, the changes observed in wet–dry-treated specimens were observed mainly owing to polymer reorganization in amorphous parts of the fibers.


**Key words:** accessibility; hornification; mechanical properties; regenerated cellulose; structure

## INTRODUCTION

During textiles manufacturing, from fiber to yarn and fabric, the material passes through stages of pretreatment, coloration, and finishing. These procedures and also care operations performed by consumers are mainly executed in aqueous environments. Herein, material is subjected to the number of succeeding steps of wetting and drying (w–d).

When cellulosic fibers are wetted, water molecules directly interact with hydroxyl groups of the cellulose chains and change the arrangement of chains by expanding the cellulose structure. As long as swelling of the crystalline parts can be excluded, the chain rearrangement is limited to amorphous parts in the fiber.[1] In the expanded structure, cellulose chains can achieve higher mobility particularly in the amorphous—low-ordered parts of fibers. Similar to the processes in heat setting, the rearrangement of the polymer chains in swollen state allows the fiber polymers to achieve lower energy.[2] When water is removed by drying, voids or interlamellar spaces collapse. As the cellulose polymer chains rearrange to a more stable state, the material will not attain the same levels of expansion upon rewetting. Similar situation can be found after thermal removal of bound water from the cellulose substrate.

The limited re-expansions on rewetting after drying are attributed to either noncovalent interactions (e.g., formation of hydrogen bonds) between fibrils, or covalent interactions such as the formation of lactone bridges between hydroxyl and carboxylic groups in the polymer chains.[3,4] Hornification has also been attributed to drying-induced crystallization in cellulosics.[5]

Pretreatment processes, for example desizing, scouring, alkali swelling treatment, and surface modification, prepare material for next wet processing during which material is dyed and treated by chemicals (softeners, hand builders, easy-care, repellent, soil-release, flame and retardant finishes, etc.) to achieve desired properties.[6] Any structural changes in fibers owing to cycles of wetting and drying will impact the accessibility of reagents and may also alter reactivity of fibers. Efficient chemical functionalization will be affected by the accessibility and reactivity of the material with treatment chemicals.

*Correspondence to:* T. Bechtold (textilchemie@uibk.ac.at).
Contract grant sponsor: Christian-Doppler Research Society and Lenzing AG, Austria.

Strength, abrasion resistance, and moisture sorption, properties relevant for consumers, will also be affected. Thus, the changes in fiber properties as a function of w–d cycles are of great importance for both textile chemical processing and consumer care cycles.

Most of the reported studies are related to the repeated washing and the use of fabric softener in the context of mechanical properties of fabrics,[7] influence of laundering on sensory properties,[8,9] and functional performance,[10,11] drying of textiles and factors affecting this process.[12–14] Few studies have focused on the effect of wetting–drying on porosity (dimensions, size, volume, etc.) of cellulosic fibers[4,15] and durability of cellulosic fabrics against pilling.[16,17] However, the porosity–accessibility relationships change with reagent type and type of interaction.

No research article related to the accessibility studies of w–d-treated cellulosic fabrics is currently available. In this study, a set of molecular probes was applied to investigate sorption properties and reactivity as a function of accessibility. Methods such as iodine sorption,[18,19] water vapor sorption, water retention value (WRV), and iron complexation,[20,21] required to characterize changes occurring in the amorphous parts were employed. Simple, sensitive, and direct methods provided a new insight into structural changes resulting from repetitive w–d treatment of three cellulosic fibers. Furthermore, the effect of w–d treatments on the molecular weight and the mechanical properties of fibers were examined. This article concentrates on lyocell (CLY) manufactured by direct dissolution of cellulose in a solution of hot *N*-methylmorpholine-*N*-oxide; viscose (CV) obtained by the treatment of cellulose with carbone disulfide and high wet modulus modal (CMD) fiber, resulting from modified CV process.[22] These fibers are of cellulose II crystalline arrangement[23] with diameter of macrofibrils in the order of 0.5–1 μm and microfibrils of 100 nm.[24]

## EXPERIMENTAL

### Chemicals and materials

$(NH_4)_2Fe(SO_4)_2{\cdot}6H_2O$, NaOH, HCl, $NH_4Ac$, AcOH, $NH_2OH.HCl$, 1,10-phenanthroline chloride(monohydrate), $Na_2S_2O_3$ (Merck, Germany), $I_2$ (Carl Roth GmbH+Co, Germany), KI, and $Na_2SO_4$ (Zeller GmbH, Austria) were analytical grade chemicals. Iron-D-gluconate (Johnson Matthey, Germany) with more than 97% purity and $P_2O_5$ (Carl Roth GmbH+Co, Germany) with more than 98.5% purity were used.

Regenerated cellulosic fibers, kindly supplied by Lenzing AG, were used in this investigation: (TENCEL® Standard)—CLY; (Lenzing Viscose®)—CV; and (Lenzing Modal® Standard)—CMD. The fineness of fibers was 1.3 dtex and their length was 39 mm.

The statistical analysis of the data was performed with the SPSS® software at a 0.05 level of significance.

### Methods

#### Wet–dry treatment

The fibers were immersed in deionized water for 15 h at 40°C and subsequently dried for 4 h at 105°C. One cycle of w–d treatment comprised one combination of wetting and drying. Fibers were subjected to 0, 5, 10, 15, and 20 w–d treatments.

All treated samples were conditioned for over 48 h in a standard atmosphere at 20 ± 2°C and 65 ± 2% relative humidity (RH) prior to the tests.

#### Microscopy

Photomicrographs of fibers before treatment and after 20 w–d cycles were recorded on a light microscope Olympus® CX41, Japan with attached digital camera Olympus® XC50.

#### Water retention values

About 0.50 g of specimen was accurately weighed and immersed in deionized water for 24 h at ambient temperature, then removed and centrifuged at 2792 × *g* for 10 min. The specimens were weighed ($W_w$) and subsequently dried in an oven for 4 h at 105°C, allowed to cool in a desiccator over powdered $P_2O_5$. Dried specimens were transferred from a desiccator directly to the balance pan such that the dry weight ($W_d$) of specimens was recorded within maximum of 10 s after removing from desiccators to minimize the exposure of samples to an ambient air humidity. During the weighing of dry specimens, the mass remained steady. The WRV in g/g was calculated according to eq. (1). Three replicate measurements per sample type were performed.

$$\mathrm{WRV} = \frac{W_w - W_d}{W_d} \tag{1}$$

To quantify the degree of structural changes the hornification index *H*, according to Racz and Borsa (eq. (2)) was used.[25]

$$H\,[\%] = \frac{\mathrm{WRV}_0 - \mathrm{WRV}_i}{\mathrm{WRV}_0} \cdot 100 \tag{2}$$

where $WRV_0$ is the water retention value of untreated fibers (g/g), $WRV_i$ is the water retention value of fibers subjected to w–d treatment ($i = 5, 10, 15, 20$) (g/g).

### Iodine sorption value

The iodine sorption capacity of the samples was measured according to a method described by Nelson et al.[18] The iodine sorption value (ISV) in mg $I_2$ per gram cellulose was calculated according to eq. (3).

$$\mathrm{ISV} = \frac{(T_s - t_s) \cdot N \cdot F \cdot 126.91}{W} \tag{3}$$

where $T_s = T_b \frac{I_s}{I_b}$ is the amount of $Na_2S_2O_3$ solution equivalent to initial iodine in aliquots of sample solution (mL), $I_s$ the mass of concentrated $I_2$-KI solution in a sample solution (g), $I_b$ the mass of concentrated $I_2$-KI solution in a blank solution (g), and $T_b$ the amount of $Na_2S_2O_3$ solution for aliquot of blank solution (mL). The variable $t_s$ denotes the amount of $Na_2S_2O_3$ solution for the aliquot of supernatant filtered from the sample (mL), $F$ the aliquot factor considering that the total volume of sample solution was 102 mL, $N$ the concentration of $Na_2S_2O_3$ (mol/L), *126.91* is the atomic mass of iodine (g/mol), $W$ the mass of sample after drying (g).

### Attenuated total reflectance-Fourier transform infrared spectroscopy

Attenuated total reflectance-Fourier transform infrared spectroscopy (ATR-FTIR) was performed at three different points of the sample using a PerkinElmer Spectrum BX spotlight spectrophotometer with a diamond ATR attachment. Scanning was conducted from 4000 to 600 $cm^{-1}$ with 64 scans for the sample as well as for background. The resolution was 4 $cm^{-1}$ and scanning interval was 2 $cm^{-1}$. Obtained spectra were normalized to the absorbance of the O—H in-plain deformation band at 1336 $cm^{-1}$.

### Dynamic water vapor sorption/desorption

The detailed settings of the instrument and procedure of measurement are the same as described earlier.[27,28] In brief, the measurement was carried out with an automatic multisample moisture analyzer SPS11-10µ (Project-Messtechnik, Ulm, Germany) at 25°C. The automate works with an analytical balance (resolution, 10 µg) and records mass changes of samples under precisely controlled temperature and humidity conditions. The atmosphere in the analyzer at the beginning of the measurement was conditioned at 0% RH and the moisture condition was increased in 10% RH steps up to 90% RH. Thereafter, the atmospheric moisture content was decreased and equilibrated stepwise at 10% RH intervals down to 0% RH. The mass change of the sample was recorded every 8 min. The equilibrium condition was set to <0.02% total mass change within 40 min and when this limit was reached the RH was automatically changed by 10%.

The Brunauer–Emmett–Teller (BET) eq. (4) was used for the determination of the water amount adsorbed as a monomolecular layer on the surface of material.[28]

$$\frac{x}{V(1-x)} = \frac{1}{V_m C} + \frac{(C-1)x}{V_m C} \tag{4}$$

where $V_m$ is the moisture regain (MR) in % corresponding to a monomolecular layer, $x$ the partial water vapor pressure, $V$ the MR in % at $x$. $C$ is the constant, which is approximately equals to exp([$E_1$-$E_L$]/RT), where $E_1$ is the heat of adsorption on the first and $E_L$ that on the succeeding layers.

### Fe-cellulose complexation

A detailed procedure of this method has been described previously.[20,21] Three replicate measurements per sample type were performed.

Freundlich (eq. (5)) and Langmuir (eq. (6)) adsorption isotherms were fitted to the equilibrium data using the software TableCurve 2D v5.0 for nonlinear regression curve fitting. While Freundlich isotherm suggests heterogeneous surface energy and does not restrict to the formation of a monolayer, Langmuir isotherm assumes equal adsorption energy for all sites.

$$C_f = K_F C_e^{1/n_F} \tag{5}$$

$$C_f = \frac{K_L C_e}{1 + a_L C_e} \tag{6}$$

where $C_e$ is the equilibrium concentration of iron in the solution (mg/L), $C_f$ the equilibrium concentration of iron in the fiber (mg/g), $K_F$ the Freundlich distribution coefficient $((\mathrm{mg/g})/(\mathrm{mg/L})^{\frac{1}{n_F}})$, $n_F$ is characterized as the affinity constant or adsorption intensity. $K_L$ is the Langmuir distribution coefficient (l/g), $a_L$ the Langmuir coefficient (L/mg).

### Tensile properties

The measurement of tensile properties of fibers was performed using Vibrodyn connected with Vibroscop (Lenzing Technik Instruments) at 20 ± 2°C and 65 ± 2% RH. The single fiber specimens under pretension of 70 mg were mounted between upper and lower jaw of a tester with gauge length 10 mm and subsequently subjected to a tensile force at 10 mm/min rate of extension until rupture. Ten repetitive measurements per sample were performed and the mean values of tenacity and elongation were plotted into the graphs.

### Wet abrasion resistance test

Twenty single fiber specimens were hung on a holder which was placed into fiber abrasion tester (DELTA 100, Lenzing Technik Instruments). A pretension of 50 mg was applied for each fiber specimen. The rotating aluminum bar with a rough surface supplied with stream of water abraded the fibers under angle 45° by rotation at a speed of 100 rpm in one direction till breaking of all specimens. Revolutions required to break each fiber specimen were automatically recorded by attached computer. Sixty replicate measurements per sample were performed and the mean values were plotted into the graphs.

### Molecular weight

The molecular weight was determined by gel permeation chromatography (GPC). To remove the softener that might hinder the dissolution process, the fibers were extracted with chloroform p.a. (Merck, Germany) in a soxhlet apparatus for 12 h. Each sample (10 mg air-dry) was suspended in 200 mL of demineralized water and shortly (two times, 10 s) mixed in a cocktail mixer. The excess water was sucked off; the sample was washed with ethanol, and subsequently placed in dry 4-mL glass vials with a tight screw cap. The vials containing the sample were left in 4 mL of DMAc (used as received) overnight. The excess DMAc was sucked off the next day and the samples were placed in dry glass vials. For dissolution DMAc/LiCl 9% (w/v) was added. After 5 days of continuous shaking pure DMAc (final ratio 2 : 3 [DMAc/LiCl 9% : DMAc]) was added. Until measurement, the samples were stored at 4°C. Directly before measurement, the samples were filtered.

GPC measurements used the following components: online degasser, Dionex DG-2410; Kontron 420 pump, pulse damper; auto sampler, HP 1100; column oven, Gynkotek STH 585; multiple-angle laser light scattering detector, Wyatt Dawn DSP with argon ion laser ($\lambda_0 = 488$ nm); refractive index (RI) detector, Shodex RI-71. Data evaluation was performed with standard Astra and GRAMS/32 software.

The following parameters were used in the GPC measurements: flow, 1.00 mL/min; columns, four PL gel mixedA LS, 20 μm, 7.5 × 300 mm; injection volume, 100 μL; run time, 45 min; *N,N*-dimethylacetamide/lithium chloride (0.9% w/v), filtered through a 0.02-μm filter, was used as mobile phase.

The amount of dissolved material was determined from the RI signal using a $dn/dc$ of 0.136 mL/g.

## RESULTS AND DISCUSSION

Conditions commonly used during technical washing and drying of fabrics entail treatment time in terms of minutes and high contact temperature (up to 160°C) or tumble drying. Household washing and drying of textiles involve high mechanical agitation for relatively short time (1–2 h) and high temperature (up to 100°C). To simulate conditions used during these two processes, samples used in this study were treated for longer time at lower temperature. The temperature for drying was selected based on the standard practice at our laboratory and prior experience. These stable gentler conditions provide scientific reproducibility and should be strong enough to show changes in fiber structure without causing mechanical damage.

### Water retention

Relative reduction in water retention is an important measure to follow the changes during wetting and drying.[3,29] The interactions of cellulosic substrates with liquid water represent the total swelling of the substrates which includes a wide expansion of the amorphous regions. The results of the WRV measurement of fully wetted fibers are summarized in Table I. The data show a significantly higher WRV for CV which exhibits the lowest crystallinity and orientation of molecules[30,31] among the studied substrates. CLY and CMD fibers show a higher restraint for swelling in water. The fibers used in this study were untreated regenerated cellulose fibers, and thus the decrease in WRV observed during the first five w–d cycles can be expected to occur during the textile dyeing and finishing operations. The changes in WRV during cycles 5–20 will be owing to consumer care operations, for example wash/dry procedures. In general, half of the overall decrease in WRV is observed to occur during the first five w–d cycles, WRV stabilize above 15 w–d cycles, which indicates low tendency of the fibers to reorganize.

The plot of the hornification index versus w–d treatment (Fig. 1) shows an increase of the hornification with increasing number of w–d treatments. All studied fibers reached a plateau at 15 w–d cycles. Generally, CLY fibers exhibited higher degree of hornification compared to CV.

The swelling conditions applied during the w–d treatment are too mild to affect the highly ordered crystalline regions considerably. Thus, the observed differences in hornification indices are related to the restructuring and reordering of amorphous parts in the fiber structure, which will influence the propensities of re-expansion of voids and interlamellar spaces on rewetting after drying.

During drying, when water evaporates, surface tension forces pull pore walls together creating internal pressures and causing them to collapse. The degree of pore closure depends on the levels of internal pressures generated, and the ability of pore

**TABLE I**
**The Changes in WRV, ISV, and BET Parameters (Surface Area, *C*) for CLY, CV and CMD Fibers Subjected to w–d Treatment**

| Substrate | Wet–dry cycles (No.) | WRV (g/g) | ISV (mg/g) | Surface area ($m^2$/g) | *C* |
|---|---|---|---|---|---|
| CLY | 0 | 0.7069 ± (0.0088)[a] | 267.6 ± 5.8 | 177.29 | 14.45 |
| | 5 | 0.5786 ± 0.0171 | 160.7 ± 10.1 | | |
| | 10 | 0.5257 ± 0.0046 | 121.7 ± 7.9 | 169.40 | 15.92 |
| | 15 | 0.4959 ± 0.0057 | 119.2 ± 0.9 | | |
| | 20 | 0.5000 ± 0.0072 | 120.5 ± 4.2 | 165.06 | 16.10 |
| CV | 0 | 0.8752 ± 0.0129 | 272.1 ± 12.2 | 198.42 | 13.49 |
| | 5 | 0.7540 ± 0.0094 | 213.7 ± 4.7 | | |
| | 10 | 0.7207 ± 0.0155 | 212.2 ± 6.3 | 192.09 | 15.05 |
| | 15 | 0.6432 ± 0.0079 | 175.2 ± 3.8 | | |
| | 20 | 0.6584 ± 0.0020 | 179.9 ± 11.4 | 188.58 | 15.70 |
| CMD | 0 | 0.6204 ± 0.0028 | 261.7 ± 12.0 | 194.26 | 15.00 |
| | 5 | 0.5438 ± 0.0082 | 214.7 ± 9.4 | | |
| | 10 | 0.5586 ± 0.0104 | 213.7 ± 11.0 | 192.50 | 15.14 |
| | 15 | 0.4309 ± 0.0254 | 142.1 ± 17.0 | | |
| | 20 | 0.4550 ± 0.0423 | 134.3 ± 6.0 | 176.25 | 17.08 |

[a] 95% Confidence intervals.

walls to resist these pressures.[32] The internal pressure is influenced by pore size and geometry, and hence hornification is likely influenced by pore shapes. The shapes of pores in CV tend to be more isotropic, that is spherical in shape compared to CLY where pores are believed to be long, elongated structures with anisotropic cross-sectional shapes.[4,33] The pores in CMD have shapes in between that of CV and CLY.[33] It is likely that the order in degree of hornification, CLY > CMD > CV, reflects the differences in pore shapes between the fiber types. Under a given level of internal pressure, the degree of collapse would be greater in anisotropic voids owing to the smaller distances between pore walls.

The higher degree of hornification of CLY and CV during the first phase of the w–d cycles can also be explained with the particular differences during fiber formation. In the CLY fiber, the cellulose chains are present in a highly oriented fibrillar structure; however, conditions during fiber spinning permitted only incomplete polymer chain rearrangement. As a result, considerable reorganization is observed during first series of w–d cycles. In production of CMD fibers, a longer time for coagulation and cellulose regeneration is permitted to achieve full mantel fibers. Lower tendency to polymer chain reorganization thus leads to a lower decrease in WRV during the first five w–d cycles.

## Microscopy

When comparing microscopic pictures of untreated and 20 w–d cycles treated fibers, it can be seen that applied treatment did not cause any mechanical damage to fibers (Fig. 2). There was no fibrillation observed typical for CLY in swollen state.[34]

## Iodine sorption, ATR-FTIR analysis

There was found no significant difference in accessibility to iodine between fiber types among untreated specimens. The w–d treatments caused a reduction in ISV for all fiber types. For CV and CMD fibers, there was a gradual and continuous reduction in ISV with increasing w–d treatments. For CLY fibers, the ISV decreased sharply up to 10 w–d treatments but did not change thereafter (Table I). Previously, it has been reported that iodine sorbs only to amorphous regions.[31] To investigate whether the changes of ISV, obtained in this article, can be attributed to the changes in crystallinity caused by w–d treatment, the crystallinity of untreated and 20 w–d-treated fiber specimens was further studied by ATR-FTIR method which has been previously employed to determine crystallinity of cellulose.[35–37]

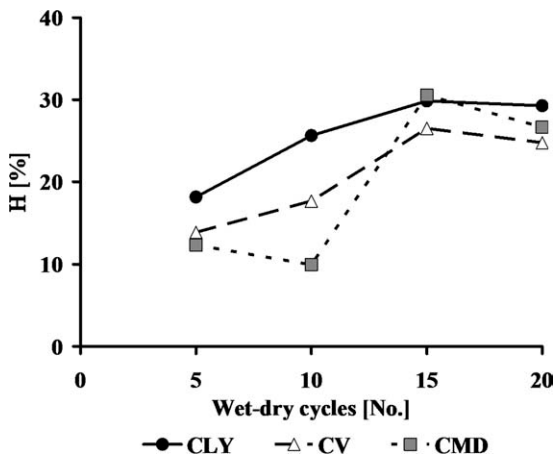


**Figure 1** Hornification index of CLY, CV, and CMD fibers subjected to w–d treatment.

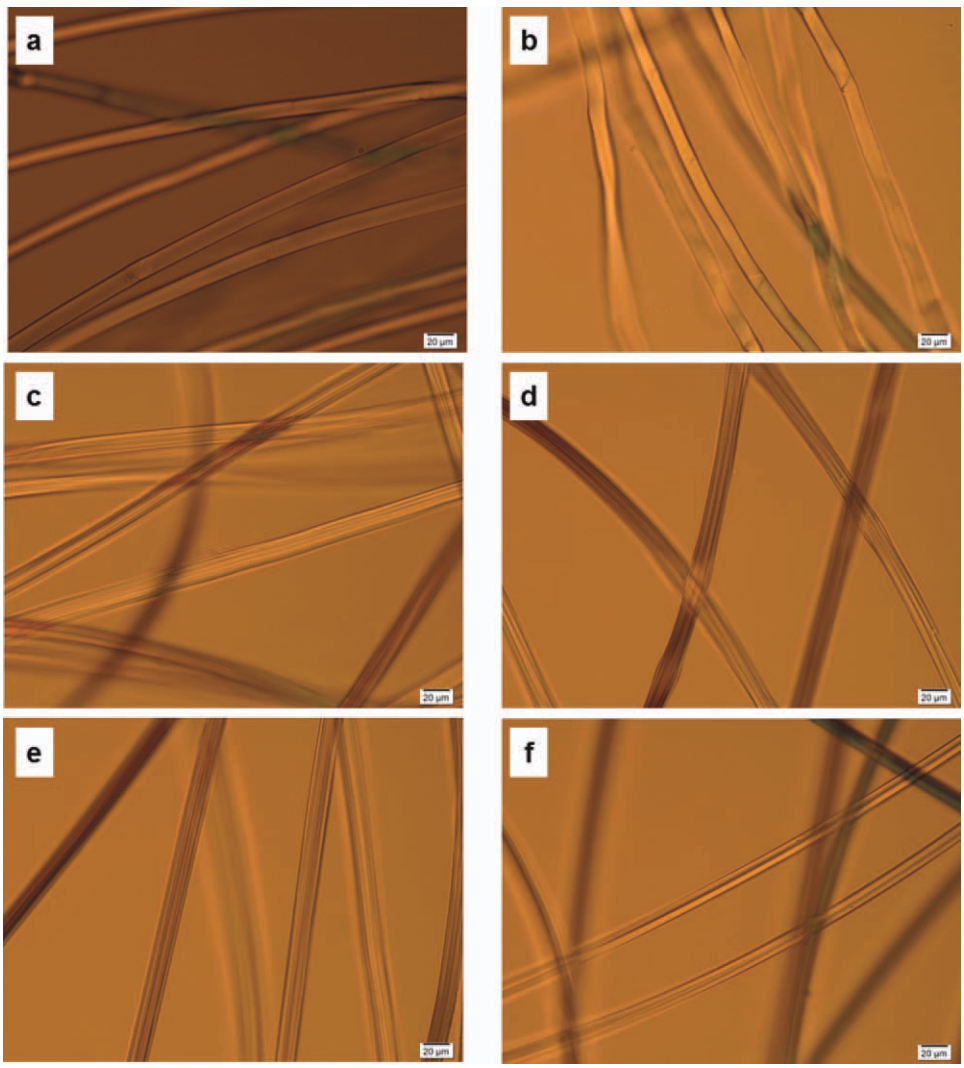


**Figure 2** Microscopic pictures of (a) CLY 0 w–d, (b) CLY 20 w–d, (c) CV 0 w–d, (d) CV 20 w–d, (e) CMD 0 w–d, and (f) CMD 20 w–d-treated fibers. [Color figure can be viewed in the online issue, which is available at wileyonlinelibrary.com.]

Total crystallinity index (TCI) and lateral order index (LOI) correlated to the crystallinity, and hydrogen bond intensity (HBI) related to the intra and intermolecular hydrogen bonds of cellulose were evaluated (Table II). TCI is the ratio of the peaks at 1366 and 2892 $cm^{-1}$, LOI the ratio of the peaks at 1418 and 894 $cm^{-1}$, and HBI 3336 and 1336 $cm^{-1}$. It can be seen that neither crystallinity nor HBI of studied fibers was influenced by w–d treatment.

Earlier studies have shown that iodine penetrates into crystalline regions when the adsorption exceeds 11–12%, and the potassium iodide, in which the iodine is dissolved, acts as a swelling agent for cellulose.[38] These factors will influence the measured ISV. Hence, the results obtained in this study confirm that ISV may be better regarded as a general measure of overall accessibility in substrates[18] and changes of this parameter are caused by reorganization of fiber internal structure.

On plotting ISV against fiber hornification, as shown in Figure 3, it is observed that the ISV decreased with rise in fiber hornification. At a given level of hornification, in the range of measured values, the ISV is observed to decrease in the general order: CV > CMD > CLY with the differences between CV and CMD tending to diminish at low levels of structural changes. These observations indicate that hornification reduces accessibility in fibers.

### Water vapor sorption

The results of the measurements of the MR at different RHs performed for untreated and w–d-treated fibers at sorption and desorption process are shown, for CLY as a representative, in Figure 4. According to the IUPAC recommendations, the isotherms could be classified from their sigmoidal shape as type II isotherms.[39] In this type of isotherms, a monolayer adsorption occurs at low water vapor pressures,

**TABLE II**
**Comparison of TCI, LOI, and HBI Obtained by ATR-FTIR for CLY, CV, and CMD Fibers**

| Substrate | Wet–dry cycles (No.) | TCI ($1366\ cm^{-1}/2892\ cm^{-1}$) | LOI ($1418\ cm^{-1}/894\ cm^{-1}$) | HBI ($3336\ cm^{-1}/1336\ cm^{-1}$) |
|---|---|---|---|---|
| CLY | 0 | 1.649 ± (0.101)[a] | 0.368 ± 0.016 | 1.225 ± 0.025 |
| | 20 | 1.589 ± 0.008 | 0.342 ± 0.010 | 1.235 ± 0.015 |
| CV | 0 | 1.478 ± 0.035 | 0.480 ± 0.021 | 1.438 ± 0.066 |
| | 20 | 1.476 ± 0.032 | 0.456 ± 0.018 | 1.466 ± 0.020 |
| CMD | 0 | 1.508 ± 0.027 | 0.488 ± 0.014 | 1.433 ± 0.023 |
| | 20 | 1.427 ± 0.027 | 0.444 ± 0.013 | 1.436 ± 0.006 |

[a] 95% Confidence intervals.

whereas a multilayer sorption occurs at high pressures. Although such isotherms are primarily used to describe sorption on materials with rather uniform surface, the sorption on cellulose materials with their highly porous structure is more complex, more similar to a swelling gel than to sorption on hard defined surfaces. The water molecules are initially adsorbed directly onto the accessible hydroxyl groups in less ordered regions, pores, and on the fibrillar surfaces. During the first phase of sorption, water molecules preferentially occupy sites which offer high adsorption energy, followed by an indirect adsorption where water molecules add onto the molecules already adsorbed, creating additional water layers.[23] As it has been shown from theoretical calculations, the highest sorption energy can be expected near the equatorial hydroxyl groups of the anhydroglucose units (AGUs), whereas the more hydrophobic top of the AGU unit will be less favourable for sorption. In a first phase of sorption, at lower RH, the most attractive sites in the structure will be covered. At higher RH, sorbed water molecules will either cover sites with lower adsorption energy or will contribute to formation of the second/third layers at sites where model calculations indicate long range effects in water structuring.[40] During this second phase, structural reorganization during w–d cycles will influence the sorption sites. The differences in MR are small at low relative humidities and they increase at higher RH values. There is a slight decrease in MR after w–d treatment in CLY and CV fibers. CMD fibers exhibit a more distinct decrease in MR after 20 w–d cycles. CLY fibers show a lower MR in comparison with CV and CMD. This property can be attributed to the greater amount of crystalline regions in CLY. However, there is no significant difference in MR between CV and CMD at zero w–d cycles in spite of their different crystallinities. After 20 w–d cycles, the MR of CMD is lower comparing to CV which indicates that not only crystallinity but also swelling affects the MR.[41]

The hysteresis between sorption (lower) and desorption (upper) isotherm was observed which is consistent with the behavior of other cellulosic fibers and wood.[26,27,42–44] This hysteresis exists owing to the hysteresis in breaking of crosslinks and replacing them by water molecules during absorption and subsequent reforming crosslinks during desorption.[23] Following the argumentation that sorption of water molecules will occur at sites where intensive interaction with the cellulose structure will be possible at low humidity, water is expected to be sorbed

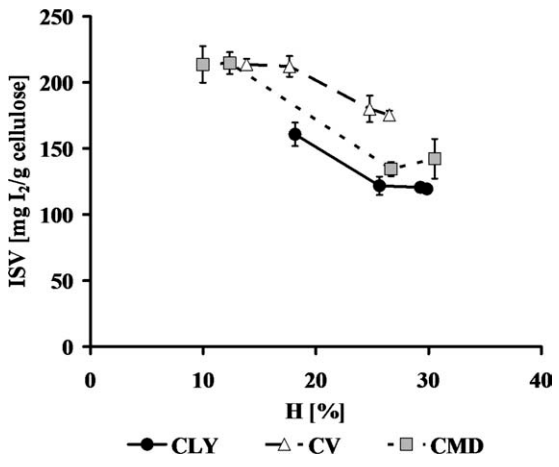


**Figure 3** The influence of hornification on ISV of CLY, CV, and CMD fibers subjected to w–d treatment.

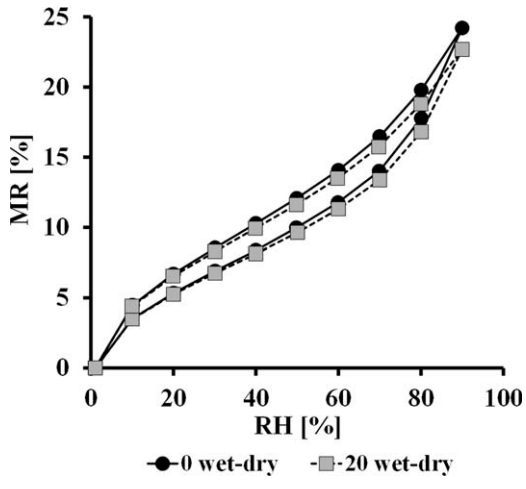


**Figure 4** Equilibrium moisture sorption/desorption isotherms of untreated and 20 w–d cycle-treated CLY fibers.

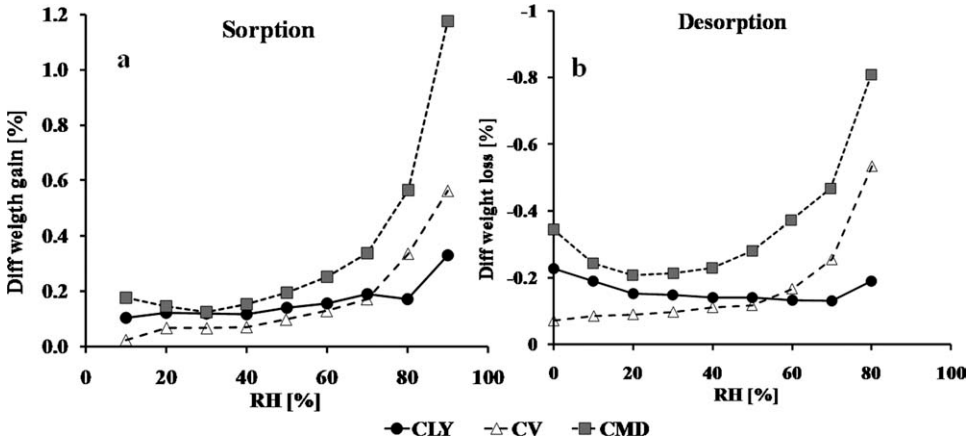


**Figure 5** Influence of w–d treatment on (a) moisture differential weight gain, and (b) moisture differential weight loss in fibers.

preferentially at highly amorphous parts of the fibrous structure. With increasing relative moisture in the surrounding atmosphere, the sorbed water will reach a level which allows local reorganization of cellulose chain segments to achieve energetically more stable forms. As a result, desorption from these sites will occur at lower RH and hysteresis will be observed in the sorption isotherm. There is a small hysteresis at low RH followed by continuous increase in the region 30–80% RH owing to the changes in surface sorption characteristics. In nonliquid state, without water condensation, mainly surface area changes owing to the reorganization of amorphous parts of fibers.

When comparing 0 and 20 w–d cycles in terms of moisture differential weight gain (for sorption) and moisture differential weight loss (for desorption), calculated from the difference $MR_{(0\ w–d)} - MR_{(20\ w–d)}$, it is obvious that these values are uniform in a wide range of RH (10–70%) for all types of fibers (Fig. 5). The highest change of moisture differential weight gain/loss was observed at high RH, where considerable amounts of water can be assumed to be present in the cellulose structure and at least local swelling can be assumed to occur, for example at RH > 70%.

Parallel exponential kinetics model has proved good fitting to sorption kinetic data for natural fibers[26,27,45–47] and wood.[48,49] Two main mechanisms of water adsorption have been suggested in the literature: cluster formation,[50,51] and multilayer adsorption.[28] Sorption of one water molecule per OH group at 92% RH has also been reported.[52] Herein, the theoretical BET isotherm analysis, exhibiting good mathematical fitting for cellulosic materials at low MR,[26,27,41] was applied. It is important to state that the situation of sorbed water in 3D cellulose structures is more complex and the fundamental assumptions of BET sorption will not be entirely valid for cellulosic materials. However, BET model allows quantification and visualization of sorption capacities and comparison of energetic aspects and thus, it can be helpful instrument to describe changes in water sorption capacities. The BET equation gives a sigmoidal isotherm, which between 0.1 and 0.5 of partial water vapor pressure is nearly linear for all studied materials. The values of $V_m$ were calculated from the slope and the intercept of this dependence and subsequently based on the known surface covered by one water molecule the total surface area was calculated (Table I). CLY fibers exhibit a significantly lower surface area in comparison with CV and CMD fibers. The observed behavior results from the fact that the surface area, based on a monomolecular adsorption layer, quantifies the overall surface area available for moisture sorption. This surface area includes pore surface area, which decreases in the order CV, CLY, and CMD.[30,31] The quantity of the surface area calculated from moisture sorption data is also determined by the amount of amorphous regions, which can absorb more water molecules than crystalline regions. According to Kreze et al.[31] the amount of amorphous regions decreases in the order CV > CMD > CLY.

The surface area decreased slightly with increasing w–d cycles for all studied fibers. Repetitive wetting and drying causes an irreversible collapse of pores and thus results in a decrease in pore volume, and also the aggregation of fibrils. Because of these phenomena, the available surface area for moisture sorption in monomolecular layer decreased.

The constant *C*, reflecting heat of sorption, was also calculated from BET model (Table I). However, no significant differences were obtained between the fibres and as a result of the w–d treatment. This is an expected behavior, as long as no chemical modification of the adsorbing surface occurs during the treatment.

### Fe-cellulose complexation

D-Gluconate is able to form very stable complexes with Fe(III) in an alkaline solution. The formed complexes of iron with sugar-type ligands have the tendency to exchange ligands in the presence of the swollen cellulose substrate which acts as a polymeric polyhydroxy ligand. As the complexation of Fe(III) ions is sensitive to changes in the cellulose structure, it was reported as a suitable method to characterize the accessibility of different fibers in the swollen state.[20,21]

The plot of the amount of iron complexated by the fibers versus the concentration of iron in the solution for untreated and w–d-treated CV fibers is shown in Figure 6 as a representative of observed behavior for all three fibers.

The overall shape of the isotherms exhibited characteristics of Langmuir adsorption isotherms, indicated by the values of the correlation coefficient ($R^2$) and the standard error. The values of $R^2$ and the standard error vary in the range of 0.9640–0.9990 and 0.051–0.207, respectively. The values of $K_L$ and $a_L$ calculated from the nonlinear regression curve fitting of the Langmuir adsorption isotherm for samples treated by 0–20 w–d cycles fall in the range of 0.125 ± 0.010–0.148 ± 0.053 l/g ($K_L$, CLY), 0.111 ± 0.006–0.134 ± 0.023 l/g ($K_L$, CV), 0.102 ± 0.017–0.134 ± 0.020 l/g ($K_L$, CMD), 0.025 ± 0.005–0.043 ± 0.021 L/mg ($a_L$, CLY), 0.017 ± 0.002–0.027 ± 0.008 L/mg ($a_L$, CV), and 0.014 ± 0.006–0.024 ± 0.006 L/mg ($a_L$, CMD). As it can be seen, there are no significant differences in $K_L$ and $a_L$ among the different fiber types and also the applied treatment did not exhibit any influence on studied parameters. These parameters are cellulose-specific properties and thus do not vary in dependency on fiber type.

Using the reported crystallinity in three fiber types,[31] an estimation of the binding capacity of the amorphous parts of the fibers can be made. If a 40% degree of crystallinity is assumed for fiber and only half of the amorphous proportion in fibers is supposed to be accessible for the reactions, the maximum iron complexation should occur in 30% of the fiber mass. The highest degree of iron complexation observed was $7.2 \times 10^{-5}$ mol Fe/g fiber; assuming 30% accessibility and all three OH groups of an AGU involved in complex formation Fe-binding capacity will be in the order of $5.6 \times 10^{-3}$ mol OH/g fiber. Thus, even if complexation reactions occurred with a 1 : 2 stoichiometry,[53,54] the observed yields of Fe-binding correspond to only 2.6% of the theoretical capacity. Thus, it is improbable that fiber saturation, characteristic of the Langmuir model, was reached in these experiments. The Freundlich model, which does not entail fiber saturation, may be better suited for the Fe complexation results, but was not found to be a good descriptor of the experimental data.

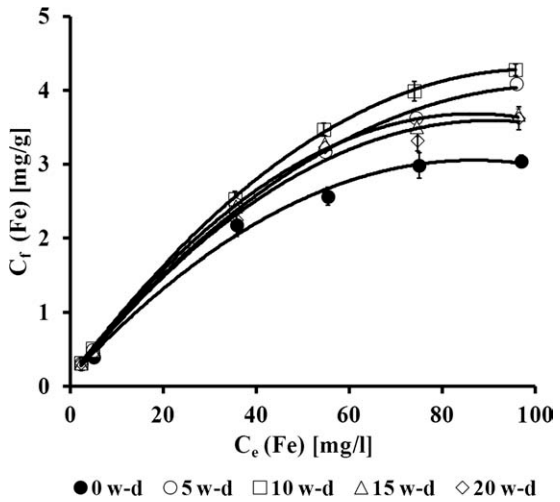


**Figure 6** Equilibrium concentration of iron in the fiber versus equlibrium concentration of iron in the solution for w–d-treated CV fibers.

CMD and CV fibers exhibited a similar binding capacity for iron, whereas that of CLY fibers was lower. The system considered here is an aqueous system containing cellulose in highly swollen state in the presence of NaOH. High swelling caused by alkali resulted into the lack of iron complexation sensitivity to the changes in the accessibility generated during w–d treatment. Hence, the repetitive w–d treatments barely affected iron accessibility of the studied fibers. Treatment in 1*M* NaOH seems to be sufficient intensive to erase/overrun the observed reorganization during w–d treatment.

### Molecular weight and mechanical properties

The influence of w–d treatment on molecular weight distribution in fibers was determined with GPC measurements. CV and CLY dissolved completely in DMAc/LiCl within time allowed for dissolution. The ease of fiber solubility decreased with increasing w–d cycles in all cases, but these effects were most pronounced for CMD fibers.

Fiber solubility is governed by degree of orientation, crystallinity, and degree of polymerization (DP), all of which are greater in CLY compared to CMD.[30,31] Owing to the poor solubility of untreated and treated CMD fibers in DMAc/LiCl which could be caused by higher overall molecular weight of the cellulose in combination with the orientation of the molecules during spinning, only the results obtained from completely dissolved samples are presented.

The molecular weight distributions are shown in Figure 7. CLY samples exhibited greater reduction of molecular weight in comparison with CV with a noticeable shift of the molecular weight distribution

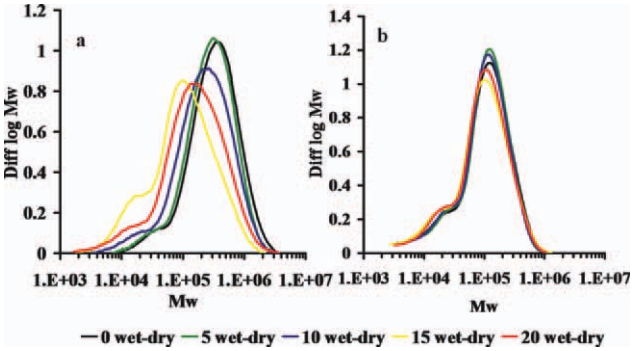


**Figure 7** Molecular weight distribution of untreated and w–d-treated (a) CLY, and (b) CV fibers. [Color figure can be viewed in the online issue, which is available at wileyonlinelibrary.com.]

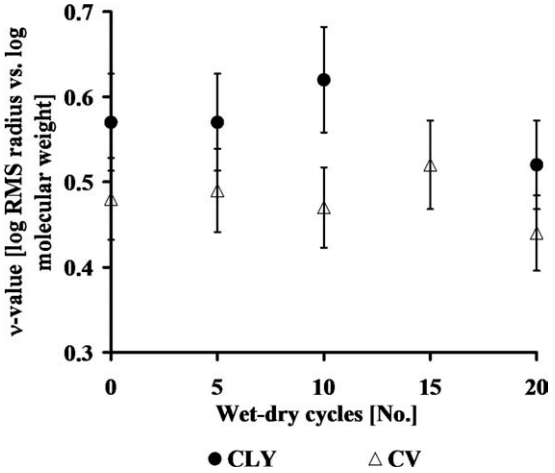


**Figure 8** Slope ν from conformation plot (log Mw versus log R<g>) of untreated and w–d-treated CLY, and CV fibers.

which was evident after only five w–d cycles. The CLY sample that was subjected to 15 w–d cycles showed a striking discontinuity compared to the other samples. More investigation is needed to find out whether this point is an outlier or reflects changes resulting from reorganization of fiber internal structure. CV samples showed a slight but clear decrease in molecular weight after 15 and 20 w–d cycles.

To get more insight into the molecules in the DMAc/LiCl solution, a double logarithmic plot of the molecular weight and the root mean square radius was used to obtain the ν-value. The lower is the ν-value the more compact is the molecule in solution. Typically, this value is between 0.5 and 0.6 for cellulose in solution.[55] This is also true for the treated cellulose fibers in this study (Fig. 8). The data for CV are in the range for the corresponding pulp. CLY exhibited greater ν-value, that is the molecules in solution are less compact, in comparison with CV. Generally, the graph shows a marginal reduction of the ν-value with increasing w–d treatment, that is the cellulose molecules from treated fibers tend to become slightly more compact in solution compared to cellulose molecules from untreated fibers.

The mechanical properties for CLY and CV were also investigated. The tenacity and elongation at break versus w–d treatment are shown in Figure 9. Tenacity and elongation of untreated fibers is directly correlated with DP, crystallinity, and orientation.[30,31] The w–d treatments reduced these parameters continuously, compared to untreated fibers, the reductions in tenacity after 20 w–d cycles are 28 and 21%, and corresponding reductions in elongation of 38 and 26% for CLY and CV, respectively.

Figure 10 shows the results of abrasion resistance test for CLY and CV fibers as a function of w–d treatments. The abrasion resistance of CV declined gradually with increasing number of w–d cycles. Low abrasion resistance of CLY can be explained by the fact that this fiber exhibits high fibrillation tendency and thus changes in the structure owing to the

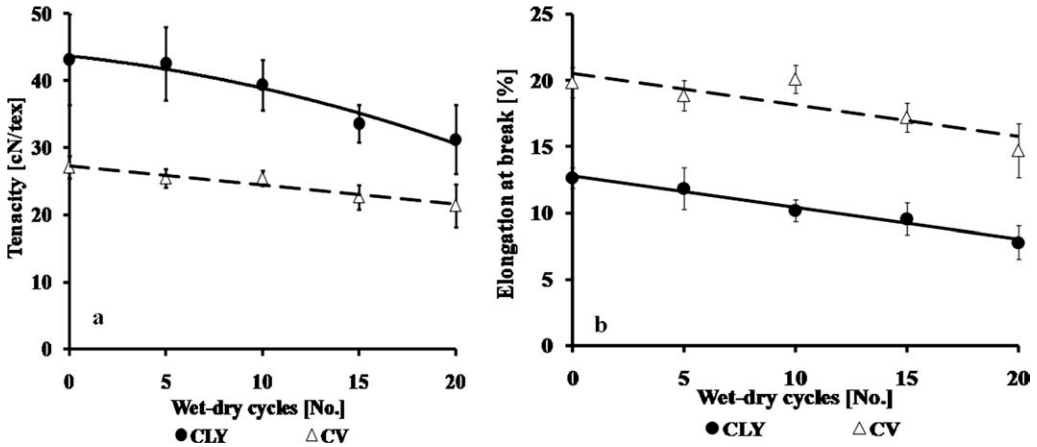


**Figure 9** Influence of w–d treatment on (a) tenacity and (b) elongation at break of untreated and w–d-treated CLY and CV fibers.

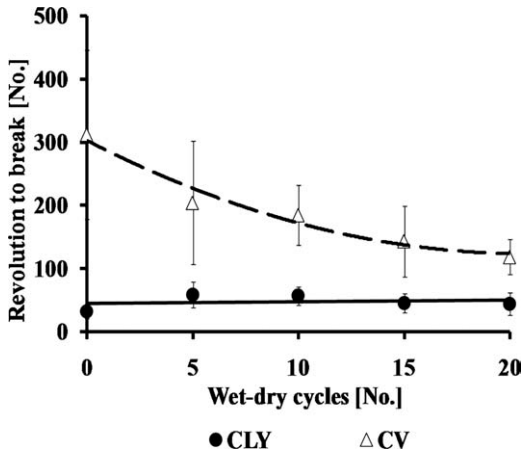


**Figure 10** Influence of w–d treatment on abrasion resistance of untreated and w–d-treated CLY, and CV fibers.

w–d treatment do not reflect in significant changes of fiber resistance.

The tenacity, elongation, and abrasion resistance are related to the DP, crystallinity, and orientation in fibers; and the propensity for stress distribution among fiber elements. Reduced stress distribution owing to reorganization of lower-ordered fiber parts to less flexible elements can cause "embrittlement."

In CLY fibers, the w–d treatments caused reductions in tenacity and elongation, but did not change abrasion resistance. In CV fibers, the w–d treatments caused tenacity and elongation reductions of 21 and 26%, respectively, as well as reductions in abrasion resistance of 62%.

In the results from GPC measurements, there was clear evidence of cellulose degradation owing to the treatments in case of CLY, but there were only small differences in molecular weight distribution between untreated and treated CV fibers. The distinct reduction in tenacity, elongation, and abrasion resistance of CV fibers in the absence of commensurate changes in molecular weight supports assumption of fiber embrittlement owing to reorganization of low-ordered amorphous fiber sections.

The slower rate of dissolution of treated fibers in DMAc/LiCl and the lower potential to distribute applied physical stress supports the model of molecular reorganization of the amorphous parts, which then appear after a series of w–d cycles to be more compact and inert.

## CONCLUSIONS

The results demonstrate the tendency of regenerated cellulose fibers to reorganize their internal structure during wet–dry treatments. It was observed that this treatment caused hornification, as evinced by reduction in liquid water retention capacity. The highest and lowest degrees of hornification were observed in highly crystalline CLY and low-crystalline CV fibers, respectively. Behavior of CMD fibers ranged between that of CLY and CV. Reorganization of low-ordered amorphous parts of regenerated cellulosic fibers was studied by measuring the sorption properties and reactivity as a function of accessibility. Although water vapor and iodine sorption decreased, in the presence of highly swelling solutions, for example 1*M* NaOH, no significant differences in iron sorption from Fe-D-gluconate solution were observed. The wet–dry treatments led to the reduction of mechanical properties, namely tenacity, elongation at break, and abrasion resistance. The methodologies given in this article presents useful analytical procedures to follow changes in the amorphous parts of regenerated cellulosic fibers.

The authors are grateful to Dr. Ján Široký for assistance with ATR-FTIR measurements and also to Versuchsanstalt-Textil of the HTL-Dornbirn for the use of their testing facilities.

## References

1. Heinze, U.; Wagenknecht, W. Comprehensive Cellulose Chemistry. Functionalisation of Cellulose; Wiley-VCH: Weinheim, Germany, 1998.
2. Ibbett, R. N.; Hsieh Y. Text Res J 2001, 71, 164.
3. Diniz, J. M. B. F.; Gil, M. H.; Castro, J. A. A. M. Wood Sci Technol 2004, 37, 489.
4. Crawshaw, J.; Cameron, R. E. Polymer 2000, 41, 4691.
5. Brancato, A. A. Thesis 2008, http://etd.gatech.edu/theses/available/etd-07292008–213453/unrestricted/brancato_adam_a_200812_phd.pdf (Accessed Nov 23, 2009).
6. Schindler W. D.; Hauser P. J.; Chemical Finishing of Textiles; Woodhead: Cambridge, England, 2004.
7. Agarwal, G.; Koehl, L.; Perwuelz, A.; Lee, K. S. Fibers Polym 2011, 12, 670 (via abstract).
8. Agarwal, G.; Koehl, L.; Perwuelz, A. Fibers Text East Eur 2011, 19, 100.
9. Avinc, O.; Wilding, M.; Gong, H.; Farrington, D. Fibers Polym 2010, 11, 924 (via abstract).
10. Tomsic, B.; Simoncic, B.; Orel, B.; Cerne, L.; Tavcer, P. F.; Zorko, M.; Jerman, I.; Vilcnik, A.; Kovac, J. J Sol Gel Sci Technol 2008, 47, 44.
11. Doty, K. C.; Easter, E. AATCC Rev 2009, 9, 37.
12. Lyons, D. W.; Vollers, C. T. Text Res J 1971, 41, 661.
13. Cannon, S. L.; Johnson, R. F.; Meenaghan, G. F. Text Res J 1973, 43, 423.
14. Steele, R. Text Res J 1958, 28, 136.
15. Kongdee, A.; Bechtold, T.; Burtscher, E.; Scheinecker, M. Carbohydr Polym 2004, 57, 39.
16. Okubayashi, S.; Campos, R.; Rohrer, C.; Bechtold, T. J Text Inst 2005, 96, 37.
17. Bui, H. M.; Ehrhardt, A.; Bechtold, T. J Appl Polym Sci 2008, 110, 531.
18. Nelson, M. L.; Rousselle, M. A.; Cangemi, S. J.; Trouard, P. Text Res J 1970, 40, 872.
19. Schwertassek, K. Melliand Textil 1931, 12, 457.
20. Kongdee, A.; Bechtold, T. Carbohydr Polym 2004, 56, 47.
21. Kongdee, A.; Bechtold, T. Dyes Pigments 2004, 60, 137.
22. Woodings, C. Regenerated Cellulose Fibres, 1st ed.; Woodhead Publishing Ltd in association with The Textile Institute Abington Hall: Abington, Cambridge, 2001.
23. Morton, W. E.; Hearle, J. W. S. Physical Properties of Textile Fibers; The Textile Institute: Manchester, UK, 1997.

24. Schuster, K. C.; Aldred, P.; Villa, M.; Baron, M.; Loidl, R.; Biganska, O.; Patlazhan, S.; Navard, P.; Rüf, H.; Jericha, E. Lenzing Ber 2003, 82, 107.
25. Racz, I.; Borsa, J. Cellulose 1997, 4, 293.26.
26. Okubayashi, S.; Griesser, U. J.; Bechtold, T. Carbohydr Polym 2004, 58, 293.
27. Okubayashi, S.; Griesser, U. J.; Bechtold, T. J Appl Polym Sci 2005, 97, 1621.
28. Brunauer, S.; Emmett, P. H.; Teller, E. J Am Chem Soc 1938, 60, 309.29.
29. Weise, U.; Maloney, T.; Paulapuro, H. Cellulose 1996, 3, 189.
30. Bredereck, K.; Hermanutz, F. Rev Prog Color 2005, 35, 59.
31. Kreze, T.; Jeler, S.; Strnad, S. Mater Res Innov 2002, 5, 277.
32. Park, S.; Venditti, R. A.; Jameel, H.; Pawlak, J. J. Carbohydr Polym 2006, 66, 97.
33. Schurz, J. Lenzing Ber 1994, 9, 37.
34. Öztürk, H. B.; Okubayashi, S.; Bechtold, T. Cellulose 2006, 13, 393.
35. Nelson, M. L.; O'Connor, R. T. J Appl Polym Sci 1964, 8, 1325.
36. Široký, J.; Blackburn, R. S.; Bechtold, T.; Taylor, J.; White, P. Cellulose 2010, 17, 103.
37. Corgié, S. C.; Smith, H. M.; Walker L. P. Biotechnol Bioeng 2011, 108, 1509.
38. Doppert, H. L. J Polym Sci A-2 1967, 5, 263.
39. IUPAC Recommendations Pure Appl Chem 1985, 57, 603.
40. Matthews, J. F.; Skopec, C. E.; Mason, P. E.; Zuccato, P.; Torget, R. W.; Sugiyama, J.; Himmel, M. E.; Brady, J. W., Carbohydr Res 2006, 341, 138.
41. Siroka, B.; Noisternig, M.; Griesser, U. J.; Bechtold, T. Carbohydr Res 2008, 343, 2194.
42. Urquhart, A. R.; Eckersall, N. J Text Inst Transact 1930, 21, T499.
43. Frandsen, H. L.; Svensson, S.; Damkilde, L. Holzforschung 2007, 61, 175.
44. Frandsen, H. L.; Svensson, S. Holzforschung 2007, 61, 693.
45. Kohler, R.; Duck, R.; Ausperger, B.; Alex, R. Comp Interface 2003, 10, 255.
46. Hill, C. A. S.; Norton, A.; Newman, G. J Appl Polym Sci 2009, 112, 1524.
47. Xie, Y.; Hill, C. A. S.; Jalaludin, Z.; Curling, S. F.; Anandjiwala, R. D.; Norton, A. J.; Newman, G. J Mater Sci 2011, 46, 479.
48. Hill, C. A. S.; Norton, A. J.; Newman, G. Wood Sci Technol 2010, 44, 497.
49. Sharratt, V.; Hill, C. A. S.; Zaihan, J.; Kint D. P. R. Polym Degrad Stab 2011, 96, 1210.
50. Barrie, J. A.; Platt, B. J Appl Polym Sci 1963, 4, 303.
51. Hartley, D. I.; Kamke, A. F.; Peemoeller, H. Wood Sci Technol 1992, 26, 83.
52. Berthold, J.; Desbrieres, J.; Rinaudo, M.; Salmen, L. Polymer 1994, 35, 5729.
53. Bechtold, T.; Burtscher, E.; Turcanu, A. J Chem Soc Dalton Trans 2002, 2683.
54. Pecsok, R. L.; Sandera, J. J Am Chem Soc 1955, 77, 1489.
55. Potthast, A.; Kostic, M.; Schiehser, S.; Kosma, P.; Rosenau, T. Holzforsch 2007, 61, 662.